1 **A Multi-Scale Daily SPEI Dataset for Drought Monitoring at Observation**

2 **Stations over the Mainland China from 1961 to 2018**

3 Qianfeng Wang[a, c*], Jingyu Zeng[a], Junyu Qi[b], Xuesong Zhang[b,c], Yue Zeng[a], Wei Shui[a],

4 Zhanghua Xu[a], Rongrong Zhang[a],Xiaoping Wu[a]

5 a. Fujian Provincial Key Laboratory of Remote Sensing of Soil Erosion and Disaster

6 Protection/College of Environment and Resource, Fuzhou University, Fuzhou,

7 350116, China

8 b. Earth System Science Interdisciplinary Center, University of Maryland, College

9 Park, 5825 University Research Ct, College Park, MD, 20740, USA

10 c. Joint Global Change Research Institute, Pacific Northwest National Laboratory

11 and University of Maryland, College Park, MD 20740, USA

*Corresponding author: Qianfeng Wang   **E-mail:**wangqianfeng@fzu.edu.cn

22 **Highlights:**

23 • The SPEI has been widely used to monitor and assess the drought characteristics.

24 • A multi-scale daily SPEI dataset was developed across the mainland China from

25 1961 to 2018.

26 • The daily SPEI dataset can identify the start and end day of the drought event.

27 • The daily SPEI dataset developed is free, open and persistent publicly available

28 from this study.

34

35

36

37

38

39

40

41

42

43

44

45 **Abstract:**

46 The monthly Standardized Precipitation Evapotranspiration Index (SPEI) can monitor

47 and assess drought characteristics with one month or longer drought duration. Based

48 on data from 1961 to 2018 at 427 meteorological stations across the mainland China,

49 we developed a daily SPEI dataset to overcome the shortcoming of coarse temporal

50 scale of monthly SPEI. Our dataset not only can identify the start and end dates of

51 drought events, but also can be used to investigate the meteorological, agricultural,

52 hydrological and socioeconomic droughts with different time scales. In the present

53 study, the SPEI data with 3-month scale were taken as a demonstration example to

54 analyze spatial distribution and temporal changes in drought conditions for the

55 mainland China. The SPEI data with 3-month scale showed no obvious intensifying

56 trends in terms of severity, duration, and frequency of drought events from 1961 to

57 2018. Our drought dataset serves as a unique resource with daily resolution to a

58 variety of research communities including meteorology, geography, and natural

59 hazard studies. The daily SPEI dataset developed is free, open and persistent publicly

60 available from this study. The dataset is publicly available via the figshare portal

61 (Wang et al, 2020),with https://doi.org/10.6084/m9.figshare.12568280.

62 **Key words:**

63 **SPEI, mainland China, drought, spatial-temporal, scale, meteorological data**

64

65

1. Introduction

66

67   Drought is one of the most destructive natural hazards worldwide. It can lead to

68 adverse effects on the ecological system, industrial production, agricultural practice,

69 drinking water availability, hydrological processes and water quality (Bussi and

70 Whitehead, 2020; Lai et al., 2019; Vicente-Serrano et al., 2012; Wang et al., 2014;

71 Wang et al., 2017). Drought has brought about ca. 221 billion dollars loss during 1960

72 to 2016 reported by the International Disaster Database (EM-DAT), and the drought

73 events in South Asia have influenced over 60 million residents from 1998 to 2001

74 (Agrawala et al., 2001). Unfortunately, the drought is expected to increase in

75 frequency and intensity due to the future warming air temperature (Trenberth et al.,

76 2014; Zambrano et al., 2018). The exacerbated drought conditions have promoted

77 some national legislation (such as drought preparedness and plan) to carry out the risk

78 management and adaptive strategy for drought disasters (Garrick et al., 2017).

79   The various drought types result in the difficulty of drought monitoring and

80 assessment. Drought definition is not unique. Some proposed defining drought

81 according to the water deficit (Wilhite and Glantz, 1985), while others defined

82 drought based on the period of abnormal arid conditions (Eslamian et al., 2017). The

83 popular drought can be classified into four types including (1) meteorological, (2)

84 agricultural, (3) hydrological, and (4) socioeconomic droughts (Mishra and Singh,

85 2010). The meteorological drought results from precipitation deficit or evaporation

86 increases (McKee et al., 1993). The meteorological drought can propagate into the

87 agricultural drought with the lower soil moisture availability, and it also can lead to

88   hydrological drought with lower streamflow and socioeconomic drought with lower

89   water availability (Barella-Ortiz and Quintana-Seguí, 2019; Gevaert et al., 2018).In

90   general, drought indices are normally used to monitor and assess the condition or

91   spatial-temporal characteristic of drought.

92   Many drought indices have been developed for the drought monitoring and

93   assessment, such as the Palmer drought severity index (PDSI) (Dai et al., 2004),

94   standardized precipitation index (SPI) (McKee et al., 1993), vegetation water supply

95   index (VWSI) (Carlson et al., 1994), vegetation health index (VHI) (Kogan, 2002),

96   vegetation temperature condition index (VTCI) (Wan et al., 2004), and other drought

97   indices (Men-xin and Hou-quan, 2016; Wang et al., 2015; Wang et al., 2017). PDSI

98   and SPI are the most popular drought studies worldwide (Dai et al., 2004; McKee et

99   al., 1993), however, they have some limitation. PDSI is only suitable to the

100   agricultural drought through characterizing the soil water deficit, and it cannot

101   identify the meteorological, hydrological, and socioeconomic droughts (Feng and Su,

102   2019). In addition, PDSI limits the spatial comparability of drought due to the fact

103   that it is heavily depending on data calibration (Sheffield et al., 2009; Yu et al., 2014).

104   Although the SPI can monitor and assess different drought types by multiple spatial

105   scales at the monthly time step, it only considers the precipitation factor and neglects

106   effects of evaporation stemmed from temperature and other meteorological factors

107   (Wang et al., 2014; Wang et al., 2017; Yang et al., 2018). To solve the above problems,

108   the Standardized Precipitation Evapotranspiration Index (SPEI), which considers the

109   advantage of both PDSI and SPI, was developed to monitor and assess droughts

110   (Vicente-Serrano et al., 2010). It not only accounts for the effect of evaporation on

111   drought, but also have the capability of spatial comparability and characterizing

112   different drought types with multiple time scales (Feng and Su, 2019; Wang et al.,

113   2015). SPEI has been widely used to delineate drought spatial-temporal evolution,

114   drought characteristics, and impacts of drought at the regional and global scales

115   (Mallya et al., 2016; Wang et al., 2014).

116   However, the commonly used SPEI fails to identify droughts with less than

117   one-month duration (Van der Schrier et al., 2011; Vicente-Serrano et al., 2010). With

118   the future climate change, flash droughts have been recently categorized as a type of

119   extreme climate events. Flash droughts occur along with sudden onset, rapid

120   aggravation, and sudden end of drought leading to severe influences (Pendergrass et

121   al., 2020). It is imperative for monitoring the flash droughts with the short-term

122   duration (e.g., several days). To use the sub-month resolution drought index, we have

123   developed the daily SPEI for the first time, and our daily SPEI has been used to assess

124   the drought and its impacts in previous studies (Wang et al., 2015; Wang et al., 2017).

125   The new SPEI can not only identify the drought with one-month and more than

126   one-month duration, but also monitor the drought with several days duration. In

127   addition, our new daily SPEI has filled the gap in the capability to monitor the onset

128   and duration of droughts. Our daily SPEI has similar principles with the commonly

129   used month SPEI in terms of time accumulation effects (Vicente-Serrano et al., 2010;

130   Wang et al., 2015; Yu et al., 2014). The daily SPEI data with different time scales can

131   also meet the requirement of monitoring and assessing of different drought types

132 (meteorological drought, agricultural drought and hydrological drought) at multi-time

133 scales (Wang et al., 2014).

134   The aim of this study, therefore, is to produce a long record (1961-2018) daily

135 drought index dataset for the whole mainland China. Specifically, we used the new

136 daily SPEI algorithm to produce the multi-time scale drought dataset at a daily time

137 resolution. Meteorological data with 427 stations including multi-factor (daily

138 precipitation, daily average air temperature, daily minimum air temperature, daily

139 maximum air temperature and sunshine) are used. The developed drought dataset at

140 the national scale has the potential to be sued to monitor and assess droughts and their

141 impacts for the different sectors.

142 **2. Data Sources and Methods**

143 **2.1 Data Sources**

144   Daily meteorological data from 1960 to 2018 were collected from the National

145 Meteorological Science Data Sharing Service Platform (http://data.cma.cn/). The data,

146 which have gone through quality controlling, have been used in many studies on

147 drought (Li et al., 2019; Wang et al., 2019). In total, there are 839 stations with public

148 data. To ensure continuous and complete data records, we selected 427 stations data

149 by removing stations with missing data exceeding 30 days. Meteorological variables

150 include the minimum and maximum air temperature (°C), precipitation (mm) and

151 sunshine duration (h). The sunshine duration was converted to solar radiation based

152 on the Ångström function (Chen et al., 2010; Wang et al., 2015). The station location

153   is shown in Figure 1.
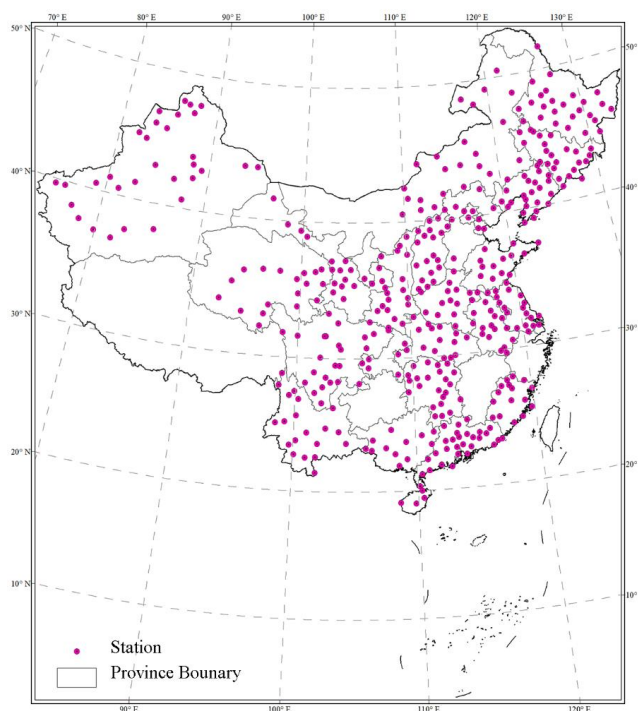
154

155   **Figure 1.** The location of meteorological stations across the mainland China.

2.2 Daily SPEI Calculation

157   The daily SPEI can be calculated by the difference between daily precipitation

158   and daily potential evapotranspiration. Because air temperature and solar radiation

159   explained at least 80% of evapotranspiration variability (Martí et al., 2015; Priestley

160   and Taylor, 1972), the Hargreaves model based on temperature and solar radiation can

161   be used to estimate the daily potential evapotranspiration (Hargreaves and Samani,

162   1982; Mendicino and Senatore, 2013; Wang et al., 2015). The daily potential

163   evapotranspiration can be obtained by the following formula:

164 $$PET = 0.0023*(T_{mean}+17.8)*\sqrt{(T_{max}-T_{min})}*R_a \qquad (1)$$

165 where, T_{mean} is the daily average air temperature ($^\circ$C); T_{max} and T_{min} are the daily

166 maximum and minimum air temperatures ($^\circ$C), respectively; and R_a is the daily net

167 radiation on the land surface (MJ m^{-2} d^{-1}).

168 SPEI calculation depends on the accumulating deficit or surplus (D_i) of water

169 balance at different time scales. D_i can be determined based on precipitations (P) and

170 PET fora given day i:

171 $$D_i = P_i - PET_i \qquad (2)$$

172 The obtained D_i values are summed at different time scales, following the same

173 procedure as that for the commonly used SPEI. The $D_{i,j}^k$ in a given day j and year

174 i depends on the chosen time scale k (days). For example, the accumulated difference

175 for 1 day in a particular year i with a 30-day (or other time scales) time scale is

176 calculated using:

177
$$X_{i,j}^k = \sum_{l=31-k+j}^{30} D_{i-1,l} + \sum_{l=1}^{j} D_{i,l} \quad , \qquad \text{if } j < k \text{ and}$$
$$X_{i,j}^k = \sum_{l=j-k+1}^{j} D_{i,l} \quad , \qquad\qquad \text{if } j \geq k \qquad\qquad (3)$$

178 We also need to normalize the water balance into a probability distribution to get

179 the SPEI index series. The best distribution for SPEI calculation is the generalized

180 extreme value (GEV) distribution (Stagge et al., 2015), which can overcome the

181 limitation of original SPEI through generalized logistic distribution for short

182 accumulation (1–2 months) periods (Stagge et al., 2015; Vicente-Serrano et al., 2010).

183 Therefore, we adopted the GEV distribution to standardize the D series into SPEI data

184 series (Monish and Rehana, 2020). The GEV probability density function is:

185
$$f(x)=\begin{cases}\left(\dfrac{1}{\sigma}\right)\left[\left(1+\xi z(x)\right)^{-1/\xi}\right]^{\xi+1}e^{-\left[(1+\xi z(x))^{-1/\xi}\right]}, & \xi\neq0,\ 1+\xi z(x)>0\\[2ex]\left(\dfrac{1}{\sigma}\right)e^{-z(x)-e^{-z(x)}}, & \xi\neq0,\ -\infty<x<\infty\end{cases}$$

186   (4)
187

where,

188    $$z(x)=\frac{x-\mu}{\sigma}$$ (5)

189

190   where, ξ,σ , and μ are the shape, scale, and location parameters respectively.

191   The cumulative distribution function $F(x)$ of GEV can be calculated by the

192   following equation:
193

194    $$F(x)=e^{-(t(x))}$$ (6)

195

where,

196    $$t(x)=\begin{cases}\left(1+\xi\left(\dfrac{(x-\mu)}{\sigma}\right)\right)^{\frac{-1}{\xi}}, & \text{if}\,\xi\neq0\\[2ex]e^{-(x-\mu)/\sigma}, & \text{if}\,\xi=0\end{cases}$$ (7)

197   Thus, the probability distribution function of the D series is given by:

198    $$F(x)=[1+(\frac{\alpha}{\chi-\gamma})^{\beta}]^{-1}$$ (8)

199   With $F(x)$, the SPEI can easily be obtained as the standardized values of $F(x)$.

200   Following the classical approximation of Abramowitz and Stegun (1965):

201    $$SPEI=W-\frac{C_0+C_1W+C_2W^2}{1+d_1W+d_2W^2+d_3W^3}$$ (9)

202   where, $W=\sqrt{-2\ln(P)}$ for $P\leq0.5$ and P is the probability of exceeding a

203   determined D value, $P=1-F(x)$. If $P>0.5$, then P is replaced by $1-P$ and the sign

205 C_2=0.010328, d_1 = 1.432788, d_2=0.189269, and d_3=0.001308.

206 **2.3 Drought Analysis Method**

207 The daily SPEI dataset were calculated at multi-time scales (1-month, 3-months,

208 6-months, 9-months and 12-months) using the daily meteorological data from

209 1960-2018 at 427 station locations. The classifications for the SPEI drought classes

210 are presented in Table 1.

211

212 Table 1 Categorization of drought and wet grade according to the SPEI.

Categorization	SPEI values
Extremely Wet	SPEI≥ 2
Severe Wet	1.5 ≤SPEI< 2
Moderate Wet	1 ≤SPEI< 1.5
Mild Wet	0.5 <SPEI< 1
Normal	-0.5 ≤SPEI≤ 0.5
Mild Drought	-1 <SPEI< -0.5
Moderate Drought	-1.5 <SPEI≤ -1
Severe Drought	-2 <SPEI≤ -1.5
Extremely Drought	SPEI≤ -2

213

214 We used the method described by Yevjevich (1967) too define the drought

215 characteristics (severity, duration, and intensity). A drought event can be firstly

216 determined by drought start and end dates, and its duration and severity were then

217 assigned. Thus, we accounted for the continuity of drought propagation. The

218 continuous days with SPEI values less than the threshold (such as -0.5,-1.0,-1.5,-2)

219 are defined as the duration of a drought event.. The severity is the integral area

220 between absolute value of the SPEI with value <-0.5 and the horizontal axis (SPEI = 0)

221   from the drought start day to the drought end day. The drought frequency is the total

222   number of drought events in a period. The drought event and its characteristics

223   (severity, duration, and intensity) can be demonstrated in Figure 2.

224
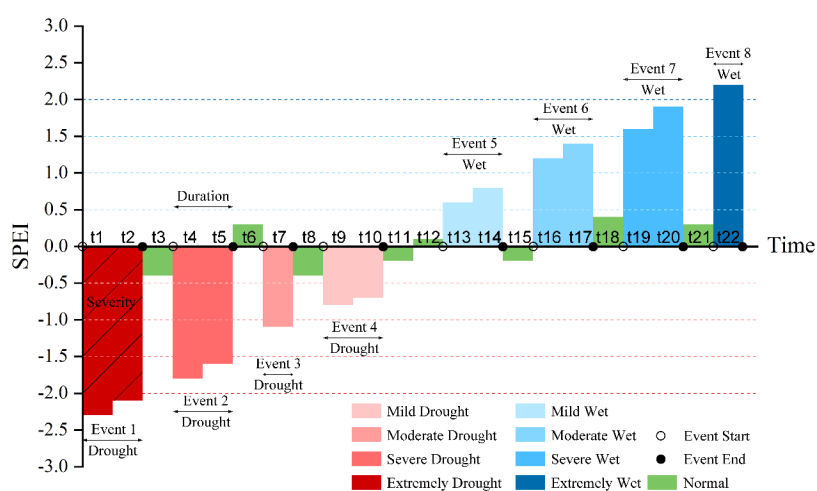
226   **Figure 2.** Schematic diagram of drought and wet events (the red shaded area

227   denotes the drought events; the blue shaded area denotes the wet events).

228

229   The SPEI data based on 90-day (3-month) time scales can be used to identify soil

230   moisture or agriculture droughts (Wang et al., 2014). Due to its important applications,

231   we selected the SPEI data with the 90-day time scales as the example data for

232   analyzing in the present study. To investigate the spatial-temporal characteristics of

233   the example data, we defined three variables including Annual Total Drought Severity

234   (ATDS), Annual Total Drought Duration (ATDD), and Annual Total Drought

235   Frequency (ATDF). The three variables were obtained by summing the severity,

236   duration, and frequency of all the drought events in each year at 427 stations.

237   We also used the non-parametric Mann–Kendall (MK) test to detect monotonic

238   trends (Kendall, 1948; Mann, 1945), and computed slopes for ATDS, ATDD and ADF

239   using the Sen's method (Sen, 1968). These statistical methods are commonly used in

240   analyses of water resources, climate, and ecology data. For the MK test, the global

241   trend for the entire series is significant when P-value < 0.05.

242   **3   Analysis Results**

243   **3.1 Spatial Distribution of Drought Characteristics**

244   The ATDS can be used to identify hot spots with severer drought conditions. Figure

245   3 shows the calculated ATDS values across the mainland China. We categorized

246   ATDS values into two main groups with higher ATDS values indicated more severe

247   drought conditions. The distribution of ATDS values shows that, in general,

248   northeastern parts of China had more severe drought conditions than southern parts.

249   However, our results also indicate that the humid climate zone in the south also

250   experienced severe drought conditions, though not as much as for northern parts of

251   China (Figure 3).

252
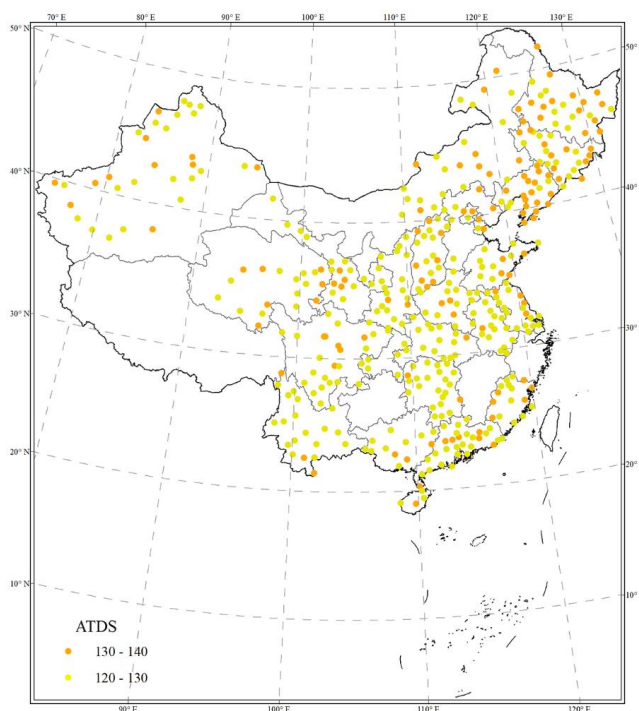
Figure 3. The spatial distribution of ATDS across the mainland China.

254

255   Figure 4 shows that ATDD values ranged from 100 to 110 days for most stations

256   across the mainland China. This indicates that there was near one-third of a year when

257   most stations were experiencing drought conditions. More stations with ATDD values

258   ranging from 100 to 110 were found compared with stations with ATDD values of

259   120-130 (Fig. 4). For drought years, the duration days of drought events are expected

260   to be were longer. The ATDD had similar spatial distribution characteristics with the

261   ATDS, indicating that droughts also occurred in the humid climate zone.

262
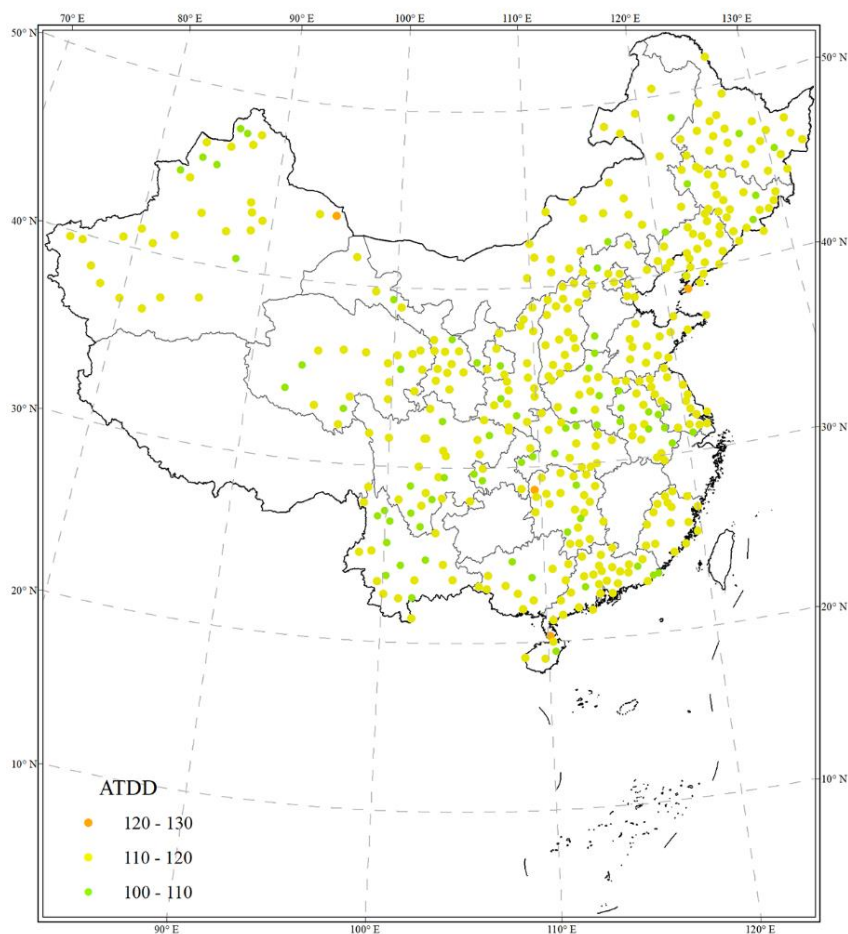
Figure 4. The spatial distribution of ATDD across the mainland China.

264

265   Figure 5 shows the spatial distribution of ATDF values across the mainland China.

266   In general, most stations had 4-6 annual drought events. There were fewer stations

267   with 6-8 annual drought events compared with stations with 2-4 annual drought

268   events. We also detected that drought events could be occurring in both arid and

269   humid regions based on spatial distributions of ATDF values (Figure 5). Since the

270   ATDF indicated only the annual average drought events, we could expect that for the

271   severer drought years the ATDF would have greater values for different stations.

272
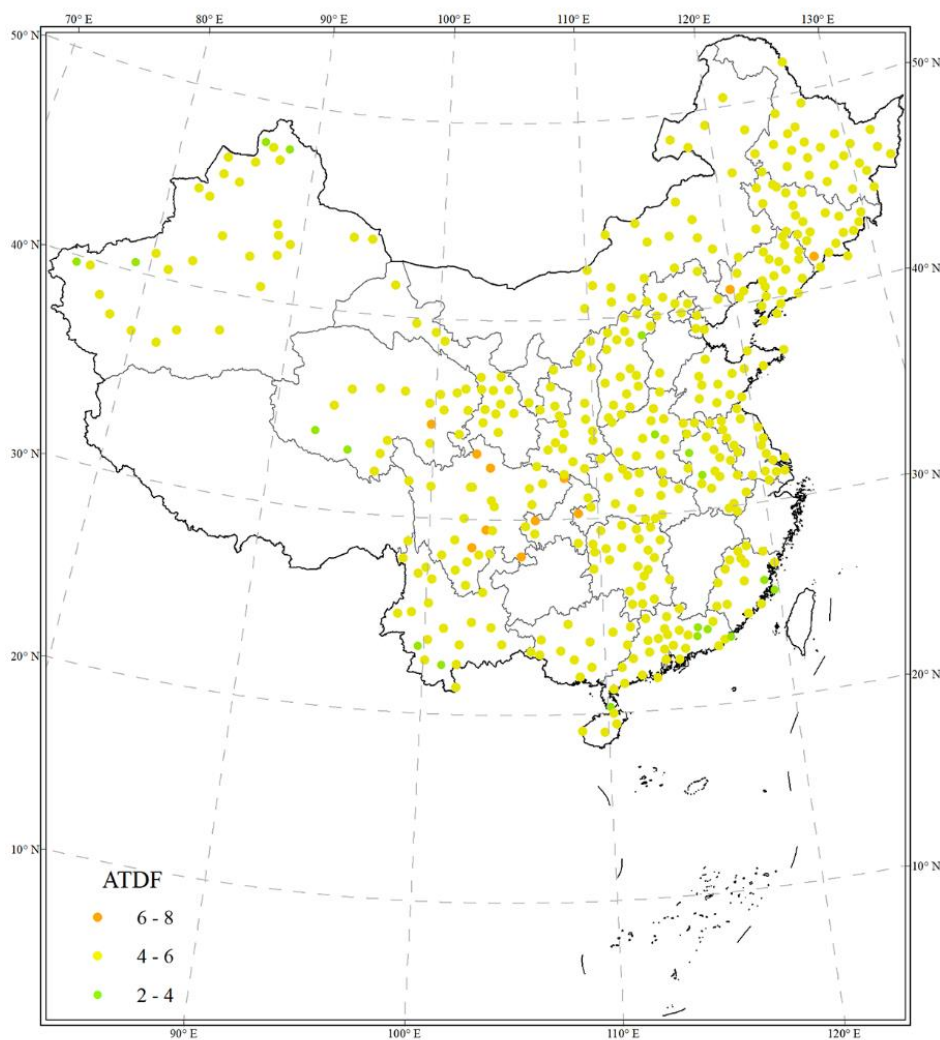
Figure 5. The spatial distribution of ATDF across the mainland China.

274

3.2 Trends in Drought Characteristics

276   The changing trends of ATDS can be used to detect whether drought severity is

277   weakening or intensifying with time, Figure 6 shows that the spatial distribution of

278   changing trends of ATDS from 1961 to 2018 across the mainland China. In general,

279   there were more stations with weakening trends in drought severity than those with

280   intensifying trends across all stations (Figure 6). It seems that both weakening and

281   intensifying absolute values were largest in the northeast, northwest, and central

282   China compared with other parts. However, after scrutiny, we found that drought

283   severity tended to weaken in the northeast, northwest, and center China with more

284   stations having significant weakening tends by statistical test (P-value<0.0.5; Figure

285   6). For southern China, most stations had no significant trends in either weakening or

286   intensifying of drought severity (P-value>0.05; Figure 6).

287
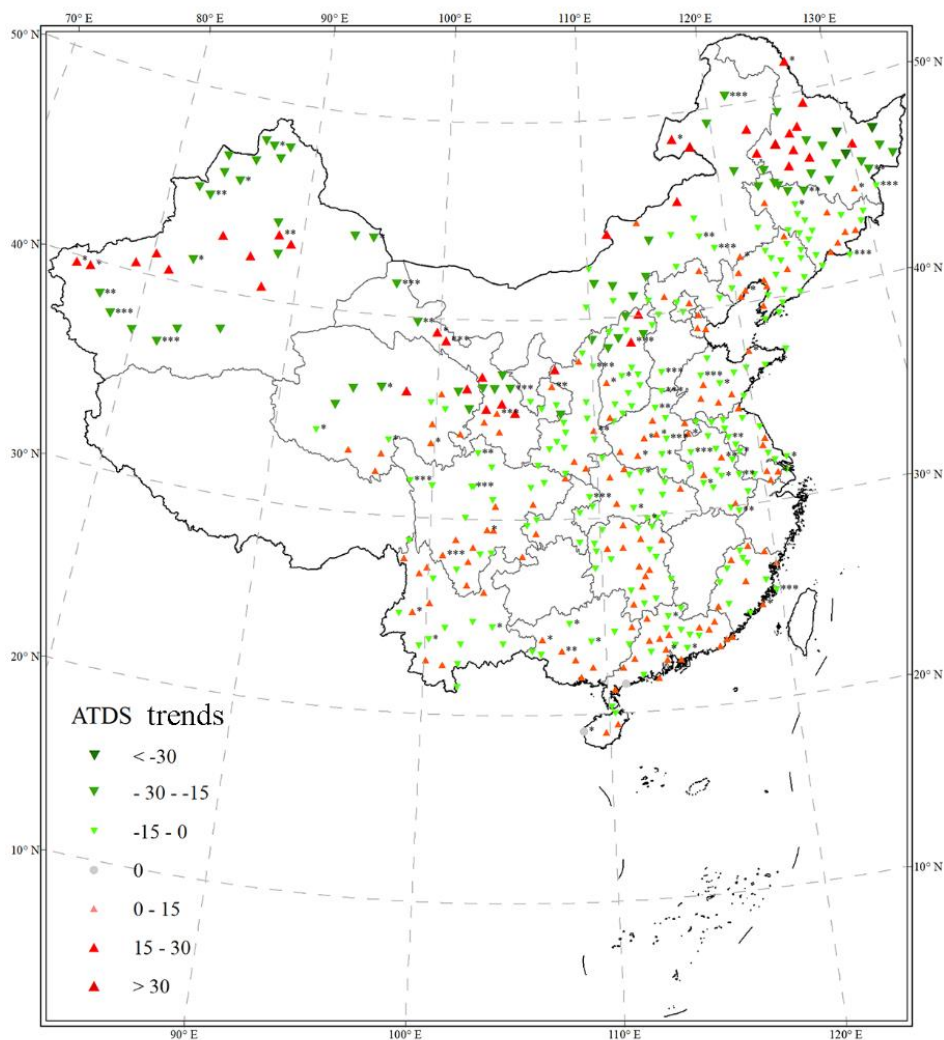
Figure 6. The spatial distribution of the changing trends of ATDS (the red and green triangular indicate increasing and decreasing trends, respectively. "***" denotes P-value < 0.001, "**" denotes P-value <0.01, and "*" denotes P-value < 0.05).

291

292   The changing trends of ATDD can be used to detect whether drought duration is

293   getting shorter or longer. Figure 7 shows the spatial distribution of changing trends for

294   the ATDD across all stations. In general, stations in the southeast demonstrated

295   downward trends with shortening drought duration, while stations in the northwest

296   had upward trends for the ATDD with increasing drought duration (Figure 7). Note

297   that the increasing or decreasing trends for ATDD were significant (P value < 0.05)

298   for stations across the central China indicating that the central China regions were

299   suffering dramatic changes of drought conditions.

300
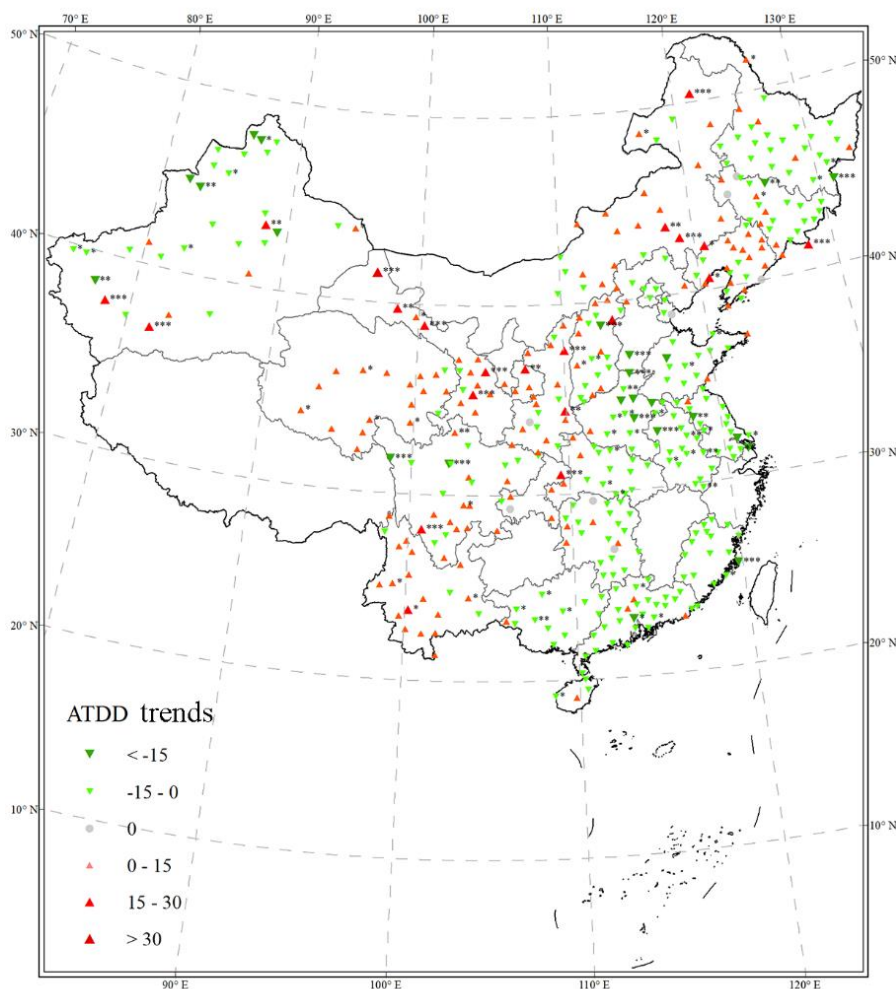
301

302   **Figure 7.** The spatial distribution of the changing trends of ATDD (the red and green

303   triangular indicate increasing and decreasing trends, respectively. "***" denotes

304   P-value < 0.001, "**" denotes P-value <0.01, and "*" denotes P-value < 0.05).

305

306   The changing trends of ATDF can be used to detect whether the frequency of

307   drought events is increasing or decreasing with time. Figure 8 shows the spatial

308   distribution of changing trends of ATDF across all stations. Most stations

309   demonstrated no significant trend in the frequency of drought events, except for

310   dozens of stations in western China having significant upward trends (P-value < 0.05)

311   with increasing frequency in drought events, and stations in northeastern China

312   demonstrated significant downward trends (P-value < 0.05) with decreasing

313   frequency of drought events.

314
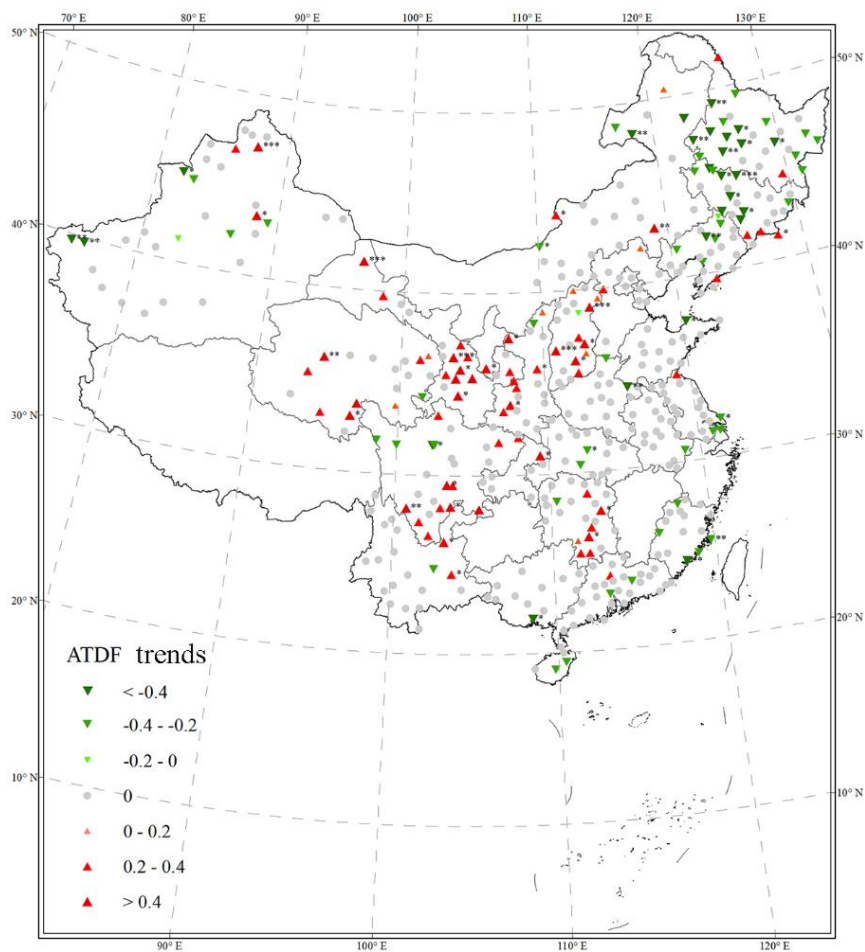
Figure 8. The spatial distribution of the changing trends of ATDF (the red and green

triangular indicate increasing and decreasing trends, respectively. "***" denotes

P-value < 0.001, "**" denotes P-value <0.01, and "*" denotes P-value < 0.05).

318

319

4. Discussion

320

321  The reason for selecting 3-month scale to assess spatial and temporal

322 characteristics of drought conditions across the mainland China is because the SPEI

323 with the 3-month scale can indicate the agricultural drought (or soil moisture) (Van

324 der Schrier et al., 2011; Wang et al., 2014; Wang et al., 2017), and its results are

325 comparable with the PDSI (Dai et al., 2004; Van der Schrier et al., 2011) and other

326 drought indices including Surface Water Supply Index (SWSI) and Moisture

327 Adequacy Index(MAI) (Doesken and Garen, 1991; McGUIRE and Palmer, 1957).

328 The commonly used monthly SPEI have been used to assess drought characteristics

329 and their impacts worldwide from the regional scale to the global scale (Stagge et al.,

330 2015; Vicente-Serrano et al., 2010; Wang et al., 2014). The SPEI with different time

331 scales is relevant for meteorological drought (1-month timescale), agricultural drought

332 (3-6-month timescale), hydrological drought (12-month timescale), and

333 socioeconomic drought (24-month timescale), respectively (Homdee et al., 2016;

334 Potop et al., 2014; Tirivarombo et al., 2018; Vicente-Serrano et al., 2010).

335  Our new SPEI dataset with multi-time scales were developed and compiled using

336 the daily SPEI algorithm in the previous study (Wang et al., 2015). The daily SPEI

337 has been used in drought monitoring and assessment, and was validated by drought

338 monitoring and assessment (Jevšenak, 2019; Jia et al., 2018; Salvador et al., 2019;

339 Wang et al., 2015; Wang et al., 2017). The global SPEI database with monthly

340 temporal resolution and 0.5 degree spatial resolution is available

341   (https://spei.csic.es/database.html). The database covers the period between January

342   1901 and December 2018. Although the database can be used effectively for the

343   meteorological, agricultural, hydrological, and socioeconomic droughts, it cannot

344   identify and detect the flash drought with less than one-month duration. In addition,

345   the database can only detect the start month and end month of drought events, and

346   therefore it fails to determine the start and end dates of a drought event, the monthly

347   SPEI (Kassaye et al., 2020; Vicente-Serrano et al., 2010; Wang et al., 2014). Our

348   newly developed daily SPEI can compensate the shortcomings of monthly SPEI in

349   drought monitoring and assessment. In addition, we used the well-received GEV

350   probability distribution for the SPEI calculation for our dataset (Stagge et al., 2015).

351   Although the daily SPEI has better performance in drought monitoring and

352   assessment (Jevšenak, 2019; Wang et al., 2017), the uncertainty of daily SPEI still

353   needs to be evaluated in future works. Our daily SPEI dataset used the simple

354   Hargreaves model based on temperature and solar radiation to estimate daily potential

355   evapotranspiration (Hargreaves and Samani, 1982; Wang et al., 2017). We will further

356   investigate effects of various evapotranspiration models (such as CRAE model,

357   Penman algorithm, Thornthwait algorithm, Makkink algorithm, and Priestley–Taylor

358   algorithm) on the calculation of SPEI (Makkink, 1957; Morton, 1983; Penman, 1948;

359   Priestley and Taylor, 1972; Thornthwaite, 1944). We only chose SPEI based on the

360   3-month timescale as an example to analyze drought characteristics, and the results

361   demonstrated that there was no obvious intensifying trends for drought across the

362   mainland China which is consistent with other studies (Han et al., 2020). Meanwhile,

363   our newly developed daily SPEI will be validated in other regions of the world.

364   Our long-term daily SPEI dataset has contributed significantly to our

365   understanding of drought evolution, especially flash drought. The dataset can be used

366   to monitor and assess different drought types (meteorological drought, agricultural

367   drought, and hydrological drought) through different timescale data. It also can

368   identify the start and end dates for drought. Our daily SPEI dataset not only have the

369   capability of monitoring and assessing droughts, but also can be used to evaluate the

370   impact of droughts on ecological system and natural resources. The dataset is valuable

371   to meteorological research and natural hazards communities for various purposes such

372   as assessment of extreme climate or drought effect evaluation.

5. Data Availability

374   All daily SPEI dataset including data and their description at 427 observed

375   meteorological stations, the data is also provided as open access via figshare (Wang et

376   al, 2020), available at doi: doi.org/10.6084/m9.figshare.12568280. This depository

377   includes the five files directory of the daily SPEI data with five scales (1 month, 3

378   month, 6 month, 12 month, 24 month) and station information for 427 meteorological

379   stations.

6. Summary

381   In the present study, we have produced a daily SPEI dataset from 1960 to 2018 at

382   427 meteorological stations across the mainland China. Our open-access dataset is an

383   important contribution to drought assessment, and it can overcome the disadvantages

384   of the commonly used monthly SPEI database. Our daily dataset can help monitor and

385   assess the spatial and temporal characteristics of droughts. It can be used to assess the

386   impacts of droughts on ecological system, hydrological processes, and other natural

387   resources. Our multi-time scale daily SPEI dataset can be widely used in studies on

388   meteorological drought (1-month timescale), agricultural drought (3-6-month

389   timescale), hydrological drought (12-month timescale), and socioeconomic drought

390   (24-month timescale). The dataset will reduce the time spent on research and avoid

391   the duplication of efforts, which will be highly attractive to meteorological,

392   geographical, natural hazard researchers and searchers from other areas.

393

394   **Author contributions.** QFW led the study, developed the method, and wrote the

395   manuscript with input from all the authors. JYQ and XSZ discussed the results and

396   revised the manuscript. All the authors contributed to the final manuscript. QFW, JYZ,

397   RRZ, XPW, and XZZ collected and analysed data over time, providing statistics and

398   material (graphs and tables) for the paper.

399

400   **Competing interests.** The authors declare that they have no conflict of interest.

401   **Acknowledgements**. This research received financial support from the National

402   Natural Science Foundation of China (41601562), the Strategic Priority Research

403   Program of the Chinese Academy of Sciences (XDA13020506) and China

404   Scholarship Council. The authors sincerely thank James Howard Stagge for his help

405 on the codes and calculation of SPEI. Special thanks go to the meteorological data

406 provider from China Meteorological Administration (http://cdc.cma.gov.cn/).

407

408 **References:**

409 Agrawala, S., Barlow, M., Cullen, H., and Lyon, B.: The drought and humanitarian

410 crisis in Central and Southwest Asia: a climate perspective, IRI special report N.

411 01-11, International Research Institute for Climate Prediction, Palisades, 24, 2001.

412 Barella-Ortiz, A. and Quintana-Seguí, P.: Evaluation of drought representation and

413 propagation in regional climate model simulations across Spain, Hydrology and Earth

414 System Sciences, 23, 5111-5131, 2019.

415 Bussi, G. and Whitehead, P. G.: Impacts of droughts on low flows and water quality

416 near power stations, Hydrological Sciences Journal, 65, 898-913, 2020.

417 Carlson, T. N., Gillies, R. R., and Perry, E. M.: A method to make use of thermal

418 infrared temperature and NDVI measurements to infer surface soil water content and

419 fractional vegetation cover, Remote sensing reviews, 9, 161-173, 1994.

420 Chen, C., Wang, E., and Yu, Q.: Modelling the effects of climate variability and water

421 management on crop water productivity and water balance in the North China Plain,

422 Agricultural Water Management, 97, 1175-1184, 2010.

423 Dai, A., Trenberth, K. E., and Qian, T.: A global dataset of Palmer Drought Severity

424 Index for 1870–2002: Relationship with soil moisture and effects of surface warming,

425 Journal of Hydrometeorology, 5, 1117-1130, 2004.

426 Doesken, N. and Garen, D.: Drought monitoring in the Western United States using a

427 surface water supply index, 1991, 10-13.

428 Eslamian, S., Ostad-Ali-Askari, K., Singh, V. P., Dalezios, N. R., Ghane, M., Yihdego,

429 Y., and Matouq, M.: A review of drought indices, Int J Constr Res Civ Eng (IJRCRE),

430 3, 48-66, 2017.

431 Feng, K. and Su, X.: Spatiotemporal Characteristics of Drought in the Heihe River

432 Basin Based on the Extreme-Point Symmetric Mode Decomposition Method,

433 International Journal of Disaster Risk Science, 10, 591-603, 2019.

434 Garrick, D. E., Hall, J. W., Dobson, A., Damania, R., Grafton, R. Q., Hope, R.,

435 Hepburn, C., Bark, R., Boltz, F., and De Stefano, L.: Valuing water for sustainable

436 development, Science, 358, 1003-1005, 2017.

437 Gevaert, A., Veldkamp, T., and Ward, P.: The effect of climate type on timescales of

438 drought propagation in an ensemble of global hydrological models, Hydrology and

439 Earth System Sciences, 22, 4649-4665, 2018.

440 Han, X., Wu, J., Zhou, H., Liu, L., Yang, J., Shen, Q., and Wu, J.: Intensification of

441 historical drought over China based on a multi-model drought index, International

442 Journal of Climatology, 2020. 2020.

443 Hargreaves, G. H. and Samani, Z. A.: Estimating potential evapotranspiration, Journal

444 of the Irrigation and Drainage Division, 108, 225-230, 1982.

445 Homdee, T., Pongput, K., and Kanae, S.: A comparative performance analysis of three

446 standardized climatic drought indices in the Chi River basin, Thailand, Agriculture

447 and Natural Resources, 50, 211-219, 2016.

448 Jevšenak, J.: Daily climate data reveal stronger climate-growth relationships for an

449   extended European tree-ring network, Quaternary Science Reviews, 221, 105868,

450   2019.

451   Jia, Y., Zhang, B., and Ma, B.: Daily SPEI reveals long-term change in drought

452   characteristics in Southwest China, Chinese Geographical Science, 28, 680-693, 2018.

453   Kassaye, A. Y., Shao, G., Wang, X., and Wu, S.: Quantification of drought severity

454   change in Ethiopia during 1952–2017, Environment, Development and Sustainability,

455   2020. 1-26, 2020.

456   Kendall, M. G.: Rank correlation methods, 1948. 1948.

457   Kogan, F.: World droughts in the new millennium from AVHRR-based vegetation

458   health indices, Eos, Transactions American Geophysical Union, 83, 557-563, 2002.

459   Lai, C., Zhong, R., Wang, Z., Wu, X., Chen, X., Wang, P., and Lian, Y.: Monitoring

460   hydrological drought using long-term satellite-based precipitation data, Science of the

461   total environment, 649, 1198-1208, 2019.

462   Li, Y., Yuan, X., Zhang, H., Wang, R., Wang, C., Meng, X., Zhang, Z., Wang, S., Yang,

463   Y., and Han, B.: Mechanisms and early warning of drought disasters: Experimental

464   drought meteorology research over China, Bulletin of the American Meteorological

465   Society, 100, 673-687, 2019.

466   Makkink, G. F.: Testing the Penman formula by means of lysimeters, Journal of the

467   Institution of Water Engineerrs, 11, 277-288, 1957.

468   Mallya, G., Mishra, V., Niyogi, D., Tripathi, S., and Govindaraju, R. S.: Trends and

469   variability of droughts over the Indian monsoon region, Weather and Climate

470   Extremes, 12, 43-68, 2016.

471 Mann, H.: Non-Parametric Tests against Trend. Econmetrica, 13, 245-259, Mantua,

472 NJ, SR Hare, Y. Zhang, JM Wallace, and RC Francis (1997), A Pacific decadal, 1945.

473 1945.

474 Martí, P., Zarzo, M., Vanderlinden, K., and Girona, J.: Parametric expressions for the

475 adjusted Hargreaves coefficient in Eastern Spain, Journal of Hydrology, 529,

476 1713-1724, 2015.

477 McGUIRE, J. K. and Palmer, W. C.: The 1957 drought in the eastern United States,

478 Mon. Weather Rev, 85, 305-314, 1957.

479 McKee, T. B., Doesken, N. J., and Kleist, J.: The relationship of drought frequency

480 and duration to time scales, 1993, 179-183.

481 Men-xin, W. and Hou-quan, L.: A modified vegetation water supply index (MVWSI)

482 and its application in drought monitoring over Sichuan and Chongqing, China,

483 Journal of Integrative Agriculture, 15, 2132-2141, 2016.

484 Mendicino, G. and Senatore, A.: Regionalization of the Hargreaves coefficient for the

485 assessment of distributed reference evapotranspiration in Southern Italy, Journal of

486 Irrigation and Drainage Engineering, 139, 349-362, 2013.

487 Mishra, A. K. and Singh, V. P.: A review of drought concepts, Journal of hydrology,

488 391, 202-216, 2010.

489 Monish, N. and Rehana, S.: Suitability of distributions for standard precipitation and

490 evapotranspiration index over meteorologically homogeneous zones of India, Journal

491 of Earth System Science, 129, 25, 2020.

492 Morton, F. I.: Operational estimates of areal evapotranspiration and their significance

493   to the science and practice of hydrology, Journal of Hydrology, 66, 1-76, 1983.

494   Pendergrass, A. G., Meehl, G. A., Pulwarty, R., Hobbins, M., Hoell, A., AghaKouchak,

495   A., Bonfils, C. J., Gallant, A. J., Hoerling, M., and Hoffmann, D.: Flash droughts

496   present a new challenge for subseasonal-to-seasonal prediction, Nature Climate

497   Change, 10, 191-199, 2020.

498   Penman, H. L.: Natural evaporation from open water, bare soil and grass, Proceedings

499   of the Royal Society of London. Series A. Mathematical and Physical Sciences, 193,

500   120-145, 1948.

501   Potop, V., Boroneanţ, C., Možný, M., Štěpánek, P., and Skalák, P.: Observed

502   spatiotemporal characteristics of drought on various time scales over the Czech

503   Republic, Theoretical and applied climatology, 115, 563-581, 2014.

504   Priestley, C. H. B. and Taylor, R.: On the assessment of surface heat flux and

505   evaporation using large-scale parameters, Monthly weather review, 100, 81-92, 1972.

506   Salvador, C., Nieto, R., Linares, C., Diaz, J., and Gimeno, L.: Effects on daily

507   mortality of droughts in Galicia (NW Spain) from 1983 to 2013, Science of The Total

508   Environment, 662, 121-133, 2019.

509   Sen, P. K.: Estimates of the regression coefficient based on Kendall's tau, Journal of

510   the American statistical association, 63, 1379-1389, 1968.

511   Sheffield, J., Andreadis, K., Wood, E. F., and Lettenmaier, D.: Global and continental

512   drought in the second half of the twentieth century: severity–area–duration analysis

513   and temporal variability of large-scale events, Journal of Climate, 22, 1962-1981,

514   2009.

515   Stagge, J. H., Tallaksen, L. M., Gudmundsson, L., Van Loon, A. F., and Stahl, K.:

516   Candidate distributions for climatological drought indices (SPI and SPEI),

517   International Journal of Climatology, 35, 4027-4040, 2015.

518   Thornthwaite, C.: Report of the Committee on Transpiration and Evaporation 1943-44,

519   Transactions of the American Geophysical Union, 25, 683-693, 1944.

520   Tirivarombo, S., Osupile, D., and Eliasson, P.: Drought monitoring and analysis:

521   standardised precipitation evapotranspiration index (SPEI) and standardised

522   precipitation index (SPI), Physics and Chemistry of the Earth, Parts A/B/C, 106, 1-10,

523   2018.

524   Trenberth, K. E., Dai, A., Van Der Schrier, G., Jones, P. D., Barichivich, J., Briffa, K.

525   R., and Sheffield, J.: Global warming and changes in drought, Nature Climate Change,

526   4, 17-22, 2014.

527   Van der Schrier, G., Jones, P., and Briffa, K.: The sensitivity of the PDSI to the

528   Thornthwaite   and   Penman-Monteith   parameterizations   for   potential

529   evapotranspiration, Journal of Geophysical Research: Atmospheres, 116, 2011.

530   Vicente-Serrano, S. M., Beguería, S., and López-Moreno, J. I.: A multiscalar drought

531   index sensitive to global warming: the standardized precipitation evapotranspiration

532   index, Journal of climate, 23, 1696-1718, 2010.

533   Vicente-Serrano, S. M., López-Moreno, J. I., Beguería, S., Lorenzo-Lacruz, J.,

534   Azorin-Molina, C., and Morán-Tejeda, E.: Accurate computation of a streamflow

535   drought index, Journal of Hydrologic Engineering, 17, 318-332, 2012.

536   Wan, Z., Wang, P., and Li, X.: Using MODIS land surface temperature and

537   normalized difference vegetation index products for monitoring drought in the

538   southern Great Plains, USA, International journal of remote sensing, 25, 61-72, 2004.

539   Wang, Q., Shi, P., Lei, T., Geng, G., Liu, J., Mo, X., Li, X., Zhou, H., and Wu, J.: The

540   alleviating trend of drought in the Huang-Huai-Hai Plain of China based on the daily

541   SPEI, International Journal of Climatology, 35, 3760-3769, 2015.

542   Wang, Q., Wu, J., Lei, T., He, B., Wu, Z., Liu, M., Mo, X., Geng, G., Li, X., and Zhou,

543   H.: Temporal-spatial characteristics of severe drought events and their impact on

544   agriculture on a global scale, Quaternary International, 349, 10-21, 2014.

545   Wang, Q., Wu, J., Li, X., Zhou, H., Yang, J., Geng, G., An, X., Liu, L., and Tang, Z.: A

546   comprehensively quantitative method of evaluating the impact of drought on crop

547   yield using daily multi-scale SPEI and crop growth process model, International

548   journal of biometeorology, 61, 685-699, 2017.

549   Wang, Q., Zeng J., Qi J., Zhang, X., Zeng, Y., Shui, W., Xu. Z., Zhang, R., Wu, X.:

550   2020: muliti-scale daily SPEI dataset over the Mainland China from 1961-2018

551   (version   June   2020),   available   at   figshare,

552   https://doi.org/10.6084/m9.figshare.12568280.

553   Wang, Y., Zhao, W., Zhang, Q., and Yao, Y.-b.: Characteristics of drought

554   vulnerability for maize in the eastern part of Northwest China, Scientific reports, 9,

555   1-9, 2019.

556   Wilhite, D. A. and Glantz, M. H.: Understanding: the drought phenomenon: the role

557   of definitions, Water international, 10, 111-120, 1985.

558   Yang, P., Xia, J., Zhang, Y., Zhan, C., and Qiao, Y.: Comprehensive assessment of

559   drought risk in the arid region of Northwest China based on the global palmer drought

560   severity index gridded data, Science of the Total Environment, 627, 951-962, 2018.

561   Yevjevich, V. M.: Objective approach to definitions and investigations of continental

562   hydrologic droughts, An, Hydrology papers (Colorado State University); no. 23, 1967.

563   1967.

564   Yu, M., Li, Q., Hayes, M. J., Svoboda, M. D., and Heim, R. R.: Are droughts

565   becoming more frequent or severe in China based on the standardized precipitation

566   evapotranspiration index: 1951–2010?, International Journal of Climatology, 34,

567   545-558, 2014.

568   Zambrano, F., Vrieling, A., Nelson, A., Meroni, M., and Tadesse, T.: Prediction of

569   drought-induced reduction of agricultural productivity in Chile from MODIS, rainfall

570   estimates, and climate oscillation indices, Remote sensing of environment, 219, 15-30,

571   2018.

572